Pharm Res (2011) 28:897–906
DOI 10.1007/s11095-010-0346-9

RESEARCH PAPER

Paclitaxel-Loaded Poly(n-butylcyanoacrylate) Nanoparticle Delivery System to Overcome Multidrug Resistance in Ovarian Cancer

Fei Ren • Ruda Chen • Ying Wang • Yabin Sun • Yaodong Jiang • Guofeng Li

Received: 29 July 2010 / Accepted: 8 December 2010 / Published online: 24 December 2010

ABSTRACT

Purpose The aim of this study was to test the ability of paclitaxel-loaded poly(butylcyanoacrylate) (PBCA) nanoparticles to overcome multidrug resistance (MDR) in human ovarian resistant cells (A2780/T) and investigate its possible mechanism.

Methods We prepared paclitaxel-loaded PBCA nanoparticles by interfacial polymerization method. The physicochemistry of the nanoparticles was characterized. The cytotoxicity of paclitaxel-loaded PBCA nanoparticles was measured by MTT assay. Calcein-AM assay was used to analyze the P-glycoprotein (P-gp) function, and the expression of MDR-1 mRNA in A2780/T cells treated with drug-loaded nanoparticles was defined by QRT-PCR.

Results The nanoparticles were approximately spherical in shape with an average diameter of 224.5 ± 5.7 nm. The encapsulation efficiency was 99.23%. The *in vitro* drug release profile exhibited a biphasic pattern. The drug formulated in PBCA nanoparticles showed a greater cytotoxicity than paclitaxel against A2780/T cells. Paclitaxel-loaded PBCA as well as blank PBCA nanoparticles decreased P-gp function in a dose-dependent manner, suggesting the efficacy of the drug-loaded nanoparticle system on overcoming MDR. There was no significant effect on inhibition to the expression of MDR1 mRNA.

Conclusions Paclitaxel-loaded PBCA nanoparticles can enhance cytotoxicity and overcome MDR through a mechanism of the inhibition of P-gp function caused by the nanoparticles system.

KEY WORDS multidrug resistance · nanoparticles · paclitaxel · P-glycoprotein function · P-glycoprotein gene expression

INTRODUCTION

As a mitotic inhibitor used in cancer chemotherapy, paclitaxel is effective for various cancers, especially breast and ovarian cancers (1,2), but its low aqueous solubility and the toxicity of the solution adjuvant (Cremophor® EL) in its commercial formulation pose formulation challenges (3,4). More importantly, paclitaxel can give rise to the multidrug resistance (MDR) that eventually leads to a clinical failure of cancer chemotherapy (5).

MDR is a complex entity involving several biochemical mechanisms, such as the over-expressions of drug efflux transporters, stress-response proteins, and anti-apoptotic factors in the tumor cells (6–8). Over-expression of P-glycoprotein (P-gp), a drug efflux transporter, is widely studied among these mechanisms. P-gp is encoded by the *mdr-1* gene and belongs to a family of energy-dependent transporters known as the ATP-binding cassette (ABC) family of proteins (9,10). It has been shown to pump substrates, including doxorubicin and paclitaxel, out of tumor cells, thus reducing the effective drug concentrations and consequently decreasing the cytotoxic activity.

F. Ren • R. Chen • Y. Sun • G. Li (✉)
Department of Pharmacy, Nanfang Hospital
Southern Medical University
Guangzhou 510515, China
e-mail: liguofeng_2010@126.com

Y. Wang
Institute of Cancer Research, Southern Medical University
Guangzhou 510515, China

Y. Jiang
Department of Urology, Nanfang Hospital
Southern Medical University
Guangzhou 510515, China

Formulation strategies like biodegradable polymer-based nanoparticles (11,12), polymeric-micelles (13) and polymer-drug conjugates (14) have been investigated to overcome P-gp-mediated drug resistance. Poly(butylcyanoacrylate) (PBCA), a biodegradable polymer, has been extensively used as an effective drug delivery system for controlled delivery of pharmacologically active moieties such as anticancer agents (15,16), antibiotics (17), peptides (18,19) and exogenous genes (20). In the 1990s, Ne´mati *et al.* reported that doxorubicin-loaded PBCA nanoparticles were able to reverse MDR at the cellular levels (21), and much attention has subsequently been given to the mechanisms by which nanoparticles reverse the MDR.

Previous studies have shown that the reversion of MDR by doxorubicin-loaded PBCA nanoparticles may result from the adsorption of the nanoparticles to the cell surface as well as from the increased doxorubicin diffusion by the accumulation of ion pairs on the plasma membrane (22). In a more recent report by Dong *et al.* (23), paclitaxel-loaded lipid-based nanoparticles exhibited a greater cytotoxicity than the free drug in P-gp-overexpression cells, which was attributed primarily to the incorporation of a surfactant in the nanoparticles to cause functional inhibition of P-gp and ATP depletion in the cells, in agreement with a work by Zhang *et al.* (24). According to another group's findings, anticancer drugs conjugated to polymers reversed the MDR of human ovarian carcinoma cells by a mechanism of partial inhibition of P-gp gene expression (14). Currently no agreement has been reached about the efficacy of the nanoparticle drug delivery systems on overcoming MDR by increasing the intracellular drug concentration. Some researchers depicted the reduction of MDR by raising the cellular drug accumulation (25,26), whereas a subsequent study demonstrated that the increased intracellular drug was still removed by P-gp efflux, as the nanoparticle formulations did not affect P-gp function (27,28).

Reports have been available describing the preparation of paclitaxel-loaded PBCA nanoparticles by mini-emulsion methods or anionic polymerization (15,29), but the ability of these nanoparticles to overcome P-gp-mediated MDR has not been investigated. In the current study, we prepared a paclitaxel-loaded PBCA nanoparticles using interfacial polymerization and examined their ability to overcome P-gp-mediated MDR in ovarian cancer cells *in vitro*. We also explored the mechanism of these nanoparticles, or their components, to overcome MDR in light of P-gp function and P-gp gene expression and provide more insights into the role of encapsulated drug combination in the treatment of MDR cancer. The design strategy of the paclitaxel-loaded PBCA nanoparticles is shown in Fig. 1.

METERIALS AND METHODS

Drugs and Chemicals

Paclitaxel was purchased from Tianfeng Technology (Xi'an, China). The monomer of n-butyl cyanoacrylate (BCA) was obtained from Sunkang Medical adhesive Co., Ltd., (Beijing, China). L-α-lecithin (soybean, MW 758.07) was purchased from Bo'ao Biotechnology Co., Ltd., (Shanghai, China). Dextran 70 (MW 68800) was purchased from Sigma Chemical Co., (St. Louis, Mo, USA). Chemicals and solvents used for HPLC were of the highest available grades and purchased from Burdick & Jackson Company (New York, USA).

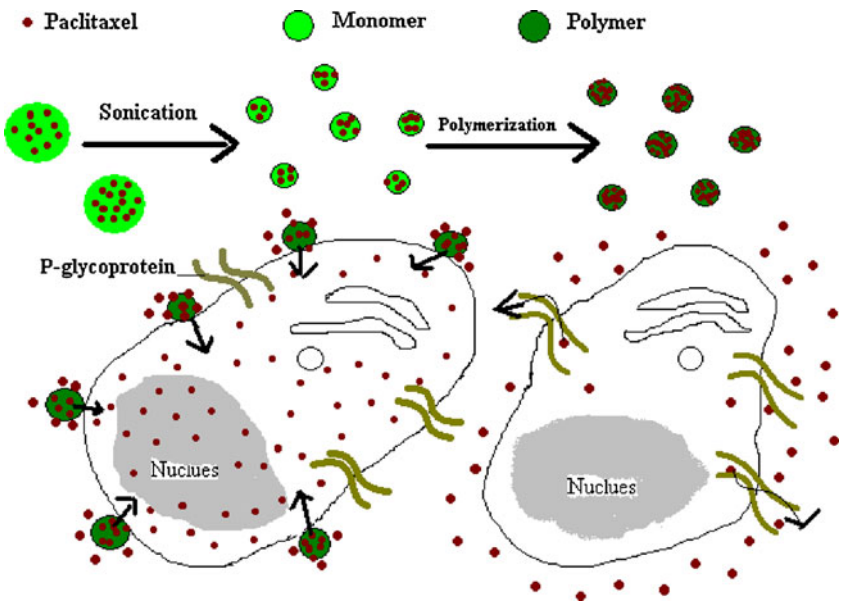

Fig. 1 Schematic illustration of the process for encapsulating drug in PBCA nanoparticles and bypassing P-gp-mediated MDR resistance.

Cells

Human ovarian carcinoma line A2780 was purchased from the Chinese Center for Type Culture Collection (CCTCC, Wuhan, China). Paclitaxel-resistant human ovarian carcinoma cell line A2780/T was obtained from American Type Culture Collection (ATCC) (Manassas, VA). A2780 and A2780/T cells were cultured in RPMI-1640 medium supplemented with 10% fetal bovine serum, penicillin and streptomycin in a humidified atmosphere of 95% air and 5% CO_2 at 37°C. The cells in exponential growth were used in the subsequent experiments.

Preparation of Paclitaxel-Loaded PBCA Nanoparticles

Paclitaxel-loaded PBCA nanoparticles were prepared by the interfacial polymerization. Briefly, 16.5 mg of paclitaxel powder was dissolved in 1 mL of acetone, in which BCA (0.1 mL, 110 mg) and glyceryl trioleate (0.05%, *v/v*) were subsequently added, followed by vortexing and sonication. The volume was adjusted to 5 mL with acetone immediately before the addition of the organic phase to the aqueous phase.

The organic solution was added in a dropwise manner to the aqueous solution (10 mL, pH 3.0) containing lecithin (1%, *w/v*) and dextran 70 (1%, *w/v*) under constant magnetic stirring (about 600 rpm) at room temperature. After 4 h of polymerization, the nanoparticle suspension was neutralized with sodium hydroxide (0.1 M) to pH 7.0 and stirred for an additional 30 min to complete the polymerization. The resulting suspension was then evaporated under a vacuum to remove acetone. The resultant suspension of the nanoparticles was filtered through a 0.45 μm membrane filter, and the nanoparticles were collected by centrifugation at 15000 rpm for 60 min and washed three times with distilled water. After lyophilization using mannitol as a cryoprotectant, the nanoparticles were stored at 4°C and resuspended with deionised water for use. The blank PBCA nanoparticles was prepared following the identical procedures, only without addition of paclitaxel during the fabrication process.

Nanoparticle Morphology and Size

The morphology of the nanoparticles was observed by field emission scanning electron microscopy (FESEM) (Quanta 400, FEI, Holland). The nanoparticles were dispersed in deionised water, and one drop of the diluted dispersion was placed on a slice of silicon. After drying, the samples were sputter-coated with a gold-palladium alloy and analyzed.

The particle size and size distribution of the drug-loaded PBCA nanoparticles were determined by dynamic laser light scattering (Zetasizer 3000, Malvern, UK) at 25°C, using scattered light at the detection wavelength of 633 nm and the angle of 90°. The nanoparticles resuspended in deionised water were diluted to a favorable concentration for better measurement. The width of the size distribution was indicated by the polydispersity index (P.D.I.).

Drug Loading and Encapsulation Efficiency

The amount of paclitaxel entrapped in the nanoparticles was detected by HPLC (Waters 2487 series, MA, USA) using a reverse-phase C_{18} column (150 mm × 4.6 mm, pore size 5 μm, Kromasil). Briefly, 5 mg of lyophilized nanoparticles were dissolved in 1 mL of methanol under vigorous stirring. The ultra-filtrates were separated by centrifugal ultrafiltration to extract free paclitaxel. The samples were then diluted with methanol, evaporated in a nitrogen atmosphere to obtain the clear solution for HPLC analysis. The resulting solution was transferred to an HPLC vial after filtering through a 0.22 μm syringe filter. The mobile phase was a mixture of acetonitrile:water (50:50, *v/v*) delivered at a flow rate of 1.0 mL/min. Paclitaxel was detected at 227 nm with an ultraviolet-visible detector. The calibration curve for paclitaxel quantification was linear over the range of standard concentration between 0.06 and 117.11 μM with a correlation coefficient of $R^2 = 0.9998$. The drug loading efficiency (L.E.) and encapsulation efficiency (E.E.) were calculated as $\text{L.E.}(\%) = (\text{amount of drug in nanoparticles}/\text{amount of nanoparticles}) \times 100\%$, and $\text{E.E.}(\%) = (\text{amount of drug in nanoparticles}/\text{initial amount of drug}) \times 100\%$.

The recovery efficiency of this extraction procedure was examined using a known weight of paclitaxel (0.01 to 0.1 mg) mixed with blank PBCA nanoparticles, and the procedure of extraction as described previously was repeated. All the recoveries were approximately 98%, suggesting that approximately 98% of the original paclitaxel could be extracted by this procedure from the mixture of paclitaxel and PBCA nanoparticles.

In Vitro Drug Release

The dialysis method was used to examine the drug release *in vitro*. The predetermined amount of lyophilized drug-loaded nanoparticles was redispersed in 5 mL of phosphate buffer solution (PBS, 0.01 M, pH 7.4) to form a suspension. The suspension was transferred into a dialysis bag (MWCO 3500) and immersed in a centrifuge tube containing 50 mL of PBS. The tube was placed in an orbital water bath shaking at 100 rpm at 37°C. After given time intervals, 1 mL of the sample was taken for analysis and replaced with fresh medium. In this study, the sink condition was maintained by frequent replacement of

fresh buffer during the *in vitro* release experiment. The newly collected samples were extracted with 2 mL of methanol and reconstituted in 5 mL of the mobile phase. The analysis procedure was similar to the measurement of E.E.

Cytotoxicity Assay

The cell viability was measured by MTT assay. A2780 and A2780/T cells were seeded in 96-well plates (8000 cells/well) containing RPMI-1640 medium supplemented with 10% fetal bovine serum (FBS). The cells were allowed to adhere for 24 h at 37°C, and the seeding medium was then removed and replaced with the experimental medium. The cytotoxicity of paclitaxel, blank PBCA nanoparticles and paclitaxel-loaded PBCA nanoparticles at increasing doses (0.01, 0.02, 0.04, 0.08, 0.16, 0.32, and 0.72 μM, equivalent concentration of paclitaxel) was determined. After 48 h of incubation in the experimental medium, the cells were incubated for another 4 h with 5 mg/mL 3-(4, 5-dimethylthiazol-2-yl) -2,5-diphenyltetrazolium bromide (MTT, 20 μL) dissolved in PBS. The clear supernatant was subsequently discarded, and the purple crystal granules were dissolved in DMSO (150 μL/well). The UV absorbance of the solubilized formazan crystals was measured using a microplate reader (Microplate reader, TECAN, Infinite M200, Austria) at 490 nm. The variation in the metabolic activity showed a good correlation to the decline of the cell growth rate. The cell viability was expressed as the ratio between the absorbance readings of the treated cells and the control cells. The dose-effect curves for determining IC_{50} values were generated using a graphical fitting method with Microsoft Excel 2003.

Calcein-AM Assay for P-gp Function

A modified calcein acetoxymethylester (calcein AM) assay was performed (30). Briefly, A2780/T cells were seeded in black 96-well plates overnight and treated with 50 μL of various doses of blank PBCA nanoparticles, paclitaxel-loaded PBCA nanoparticles and lecithin diluted in EBSS buffer for 30 min. After washing, 50 μL of fresh EBSS buffer was added, followed by the addition of 50 μL of 0.25 μM calcein AM (Sigma-Aldrich) in each well and measurement of the fluorescence of calcein using a microplate reader with 485/589 excitation/emission at room temperature. The intracellular fluorescence signal was obtained by subtracting background fluorescence of the control wells, and calcein uptake was expressed as the percentage of the control. To assess the cell membrane integrity, the cells were treated with the same samples for 0.5 h at 37°C and incubated for 1 h at room temperature. The cells were trypsinized, and 50 μL of 0.4% trypan blue solution was added. The membrane integrity was normalized to the untreated control and expressed as (viable cells / total cells) × 100%.

Quantitative RT-PCR Analysis

Following treatment of A2780/T cells with blank PBCA nanoparticles, paclitaxel-loaded PBCA nanoparticles and lecithin, as well as paclitaxel for 72 h, the total RNA was extracted from the cells using the RNAiso Plus reagent (TAKARA, Dalian, Liaoning Province, China) based on the supplier's protocol. Reverse transcription was performed at 37°C for 15 min and at 85°C for 5 s using the SYBR PrimeScriot RT-PCR Kit (Takara, Dalian, Liaoning Province, China). Quantitative RT-PCR (QRT-PCR) was performed using SYBR PrimeScriot RT-PCR Kit (Takara, Dalian, Liaoning Province, China) on a Stratagene MX3005P QRT-PCR system (Agilent Technologies, Santa Clara, USA). The primers used in the QRT-PCR reactions were as follows: β-actin, 5′-CGA GAA GA T GAC CCA GA TCA-3′ (antisense) and 5′-GA TCTTCA T GA GGTA GTCA G-3′ (sense) product size of 240 bp; MDR1, 5′-GTAC CCA TCA TT GCAA TA GC-3′ (antisense) and 5′-CAAACTTCT GCTCCT GA GTC-3′ (sense) (product size of 157 bp). The thermal cycles for PCR amplification were carried out with an initial denaturation at 95°C for 10 min followed by 40 cycles of denaturation (95°C for 15 s), annealing (60°C for 20 s) and extension (72°C for 10 s).

Statistical Analyses

One-way analysis of variance or independent sample *t*-test was carried out using a statistical program (Statistical Package for the Social Sciences, Version 13.0, SPSS Inc., USA). All the data were analyzed in qudaruplicate and presented as a mean value with its standard deviation indicated (mean ± S.E.). The means were judged to be different when $P<0.05$ and significantly different when $P<0.01$.

RESULTS

Characterization of Nanoparticles

In this study, the paclitaxel loading efficiency and encapsulation efficiency of the nanoparticles were 1.07% and 99.23% measured by HPLC, respectively. Unambiguous proof of the introduction of paclitaxel molecules in PBCA nanoparticles came from HPLC analysis (Fig. 2). Compared with blank PBCA nanoparticles, paclitaxel-loaded PBCA nanoparticles showed a paclitaxel peak at 9.732 min, which was consistent with the retention time of free

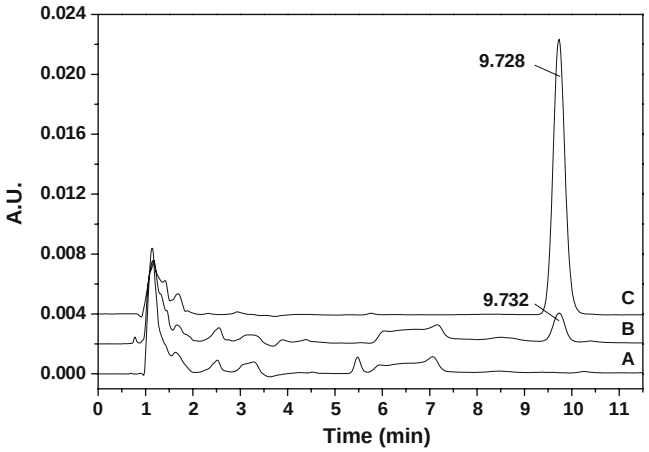

Fig. 2 HPLC chromatograms obtained from blank PBCA nanoparticles (**A**), paclitaxel-loaded PBCA nanoparticles (**B**), paclitaxel (**C**).

paclitaxel (9.728 min). As shown in Fig. 3, the paclitaxel-loaded PBCA nanoparticles observed by FESEM were spherical in shape with a diameter of 220 nm and were evenly distributed in the aqueous phase (P.D.I. = 0.27).

In Vitro Drug Release

The *in vitro* release profiles of paclitaxel from paclitaxel-loaded PBCA nanoparticles into PBS solution were presented in Fig. 4. Paclitaxel-loaded PBCA nanoparticles exhibited an initial rapid release during the first 12 h, followed by a slow release lasting till 96 h. The initial rapid release phase revealed that some of the drug was on or near the surface of nanoparticles, and the second slow release phase might be caused by paclitaxel release from the inner core of the nanoparticles. The results suggested progressive release of the drug from the paclitaxel-loaded PBCA nanoparticles, and the appropriate release rate facilitated further application of this drug delivery system.

Cell Viability of Nanoparticles

To investigate the ability of the drug-loaded nanoparticles to overcome P-gp-mediated MDR, we evaluated the *in vitro* cytotoxicity of paclitaxel-loaded PBCA nanoparticles, blank PBCA nanopartilces and free paclitaxel to parental (A2780) and resistant (A2780/T) cells by MTT assay. As shown in Fig. 5, the paclitaxel-loaded nanoparticles exhibited a dose-dependent cytotoxicity against both of the parental and resistant cell lines, and the blank PBCA nanoparticles displayed low toxicicity. Paclitaxel-loaded PBCA nanoparticles and the free drug both exhibited significant inhibition of the parental cell line A2780, and paclitaxel-loaded nanoparticles (IC_{50}: 0.08 μM) showed a 17-fold lower IC_{50} value in A2780 cells than free paclitaxel (IC_{50}: 1.39 μM). More importantly, the drug formulated in PBCA nanoparticles displayed better inhibited effects against A2780/T cells than free paclitaxel. That is, paclitaxel-loaded PBCA nanoparticles (IC_{50}: 0.13 μM) revealed 594-fold lower

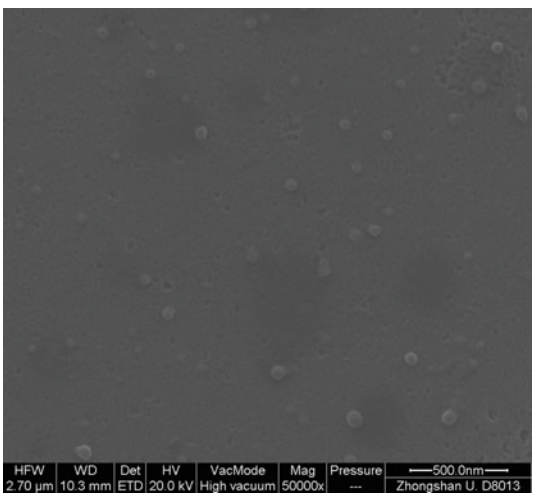

(A)

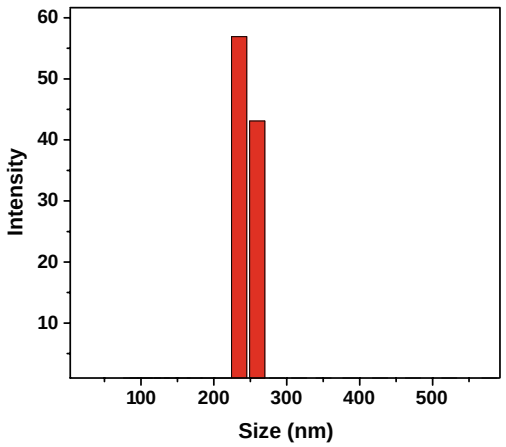

(B)

Fig. 3 Scanning electron microscopy (**A**, ×50000) and particle size distribution (**B**) of paclitaxel-loaded PBCA nanoparticles.

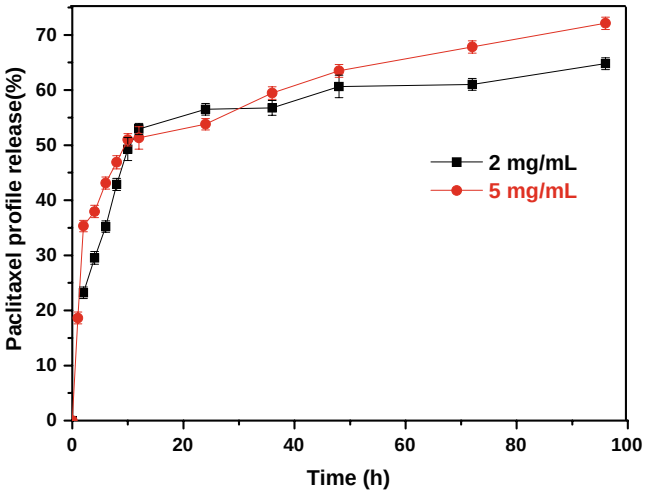

Fig. 4 Release profiles of different concentrations (2 mg/mL and 5 mg/mL) of paclitaxel-loaded PBCA nanoparticles at 37°C *in vitro*. The data are presented as mean ± S.E. ($n = 4$).

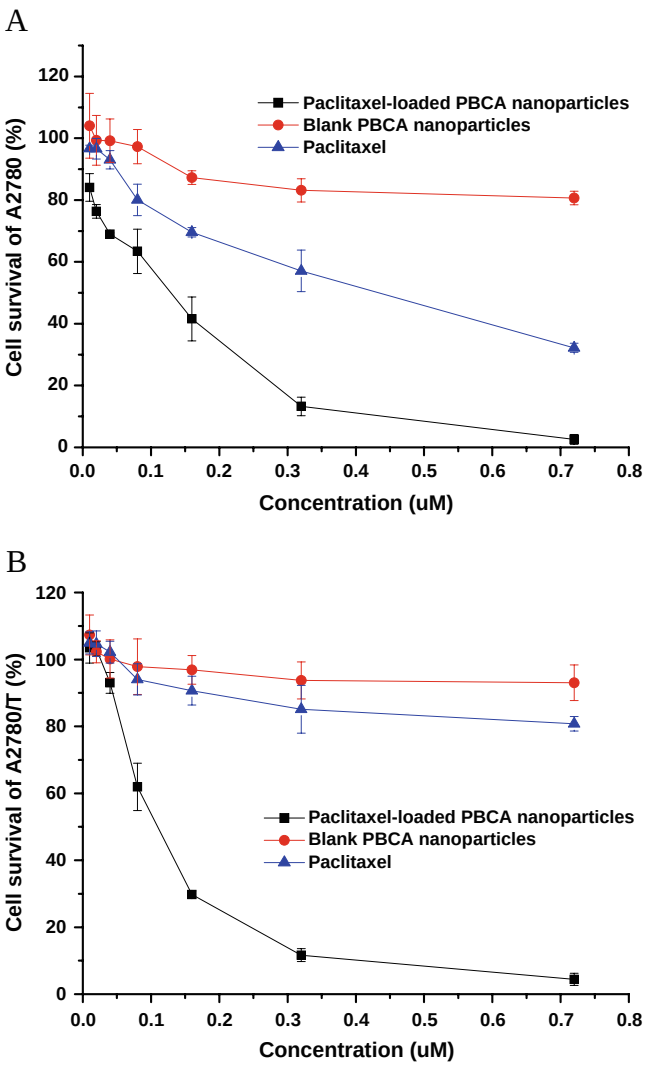

Fig. 5 Cytotoxicity of paclitaxel-loaded PBCA nanoparticles and blank PBCA nanoparticles in comparison with that of paclitaxel at the same dose against A2780 (**A**) and A2780/T cells (**B**). The data are presented as mean ± S.E. ($n = 4$).

than that of paclitaxel in A2780/T cells (IC_{50}: 77.22 μM), suggesting a greater *in vitro* cytotoxicity of paclitaxel-loaded PBCA nanoparticles than the free drug against the resistant cells.

Effect of Paclitaxel-Loaded PBCA Nanoparticles on the Uptake of Calcein AM in A2780/T Cells

To investigate the mechanisms by which drug-loaded nanoparticles, blank nanoparticles and the surfactants inhibited P-gp function, the intracellular calcein fluorescence in the resistant cells (A2780/T) was measured after a 30-min exposure to various concentrations of these samples. On account of its biocompatible and inert properties, dextran 70 was usually used as the surfactant for fabricating nanoparticles; consequently, its effect on P-gp was considered basically negligible (31). In A2780/T cells, the intracellular calcein fluorescence increased by a concentration-dependent manner after treatment with paclitaxel-loaded PBCA nanoparticles and blank PBCA nanoparticles, reaching the maximum at the highest concentration ($P<0.05$) (Fig. 6). Interestingly, the intracellular calcein fluorescence of lecithin exhibited a concentration-dependent biphasic effect. At lower lecithin concentrations (0.01–0.06 μM, corresponding to lecithin content in the nanoparticles), we observed intracellular calcein fluorescence signals below the control level, suggesting the activation of P-gp transport activity. However, as lecithin concentration increased to a level sharply higher than that in the nanoparticles (0.16 μM), the fluorescence signal exceeded the control level, indicating the inhibition of P-gp activity. Under all the conditions tested, the trypan blue assay confirmed that no significant loss of the cell membrane integrity ever occurred (data not shown).

In addition, we used verapamil (Ver) as the positive control for maximal P-gp inhibition in the experiments. With 10 μM verapamil, the calcein fluorescence signals in A2780/T cells were obviously higher than the control level ($P<0.01$).

Effect of Paclitaxel-Loaded PBCA Nanoparticles on P-gp Gene Expression in A2780/T Cells

Compared with the parental A2780 cells, the resistant A2780/T cells showed an obviously elevated expression of MDR-1 mRNA ($P<0.01$) (Fig. 7A). To further explore the inhibition mechanisms by P-gp gene expression, the expression of MDR-1 mRNA in A2780/T cells was detected after treatment with paclitaxel-loaded PBCA nanoparticles, blank PBCA nanoparticles and lecithin, as well as paclitaxel by QRT-PCR (Fig. 7B). According to the results of Calcein-AM assay, we selected the highest test concentration (0.32 μM for the free drug, drug-loaded nanoparticles, and blank nanoparticles, and 0.16 μM for lecithin) to detect the expression of MDR-1 mRNA. Although paclitaxel-loaded PBCA nanoparticles produced greater inhibition on MDR-1 mRNA expression than the free drug in A2780/T cells, they failed to result in significant differences from the expression in the control group ($P>0.05$). Meanwhile, blank PBCA nanoparticles and lecithin slightly up-regulated the expression of MDR1 mRNA, implying that blank nanoparticles and the surfactant could not obviously affect P-gp gene expression ($P>0.05$).

DISCUSSION

In this study, we prepared paclitaxel-loaded PBCA nanoparticles containing dextran 70 and lecithin as the surfactants by interfacial polymerization, which involved only one step for dispersion of the organic phase in the aqueous phase to avoid the purification procedure. The paclitaxel

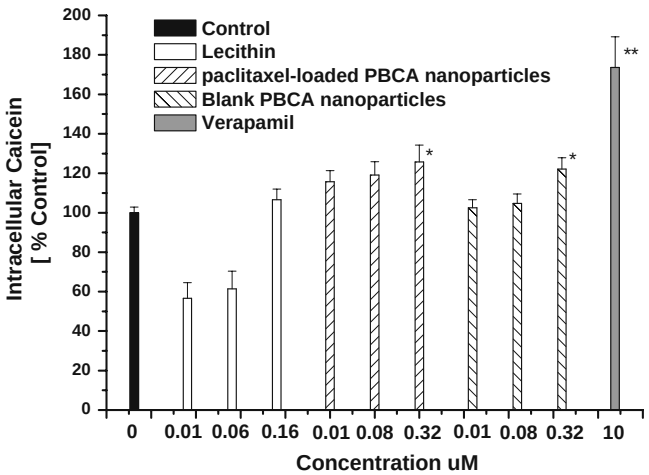

Fig. 6 Intracellular calcein accumulation in control A2780/T cells and the cells treated with verapamil, paclitaxel-loaded PBCA nanoparticles, blank PBCA nanoparticles, and lecithin. The data are presented as mean ± S.E. ($n=4$). *$P<0.05$, **$P<0.01$ *vs* the control group.

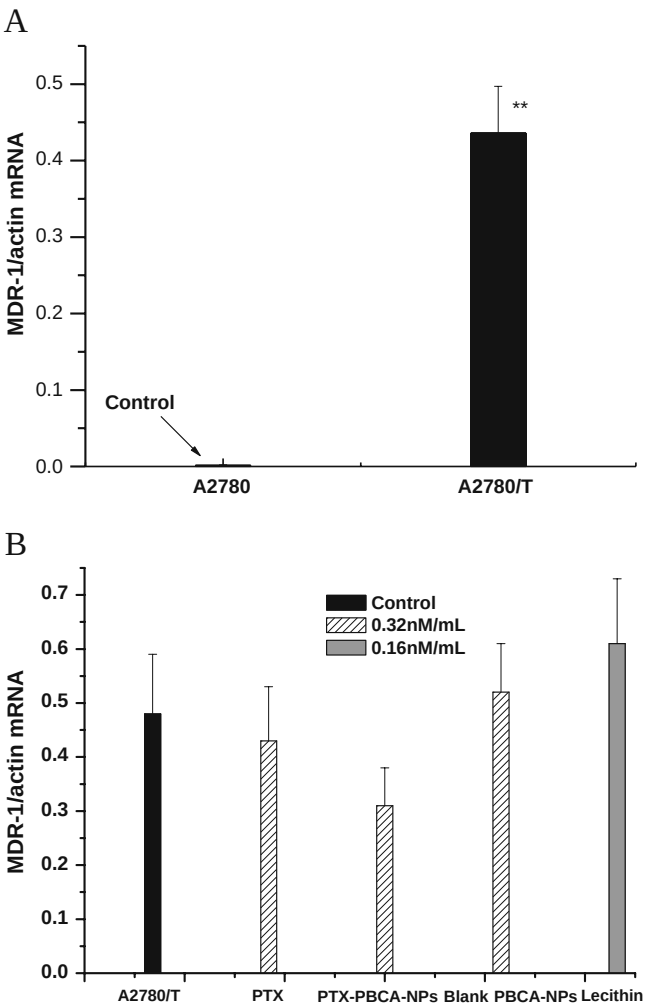

Fig. 7 Expression of MDR-1 mRNA measured by QRT-PCR in untreated A2780 and A2780/T cells (**A**) and the cells treated with the testing agents (**B**). The data are presented as mean ± S.E. ($n = 4$). $^{*}P < 0.05$, $^{**}P < 0.01$ *vs* the control group.

monomer was homogenized by sonication to obtain tiny monomer droplets, which were then converted into paclitaxel-loaded PBCA nanoparticles by the subsequent polymerization (Fig. 1). Compared with emulsion polymerization, interfacial polymerization allows high encapsulation and drug loading rates, attributable to the introduction of the surfactants such as lecithin and dextran 70. The inclusion of lecithin and dextran 70 in the formulation also renders the system more homogeneous and stable, thus facilitating further incorporation of the highly hydrophobic paclitaxel (32). The relatively high drug loading and encapsulation rates of paclitaxel in this system may also result from its high partition coefficient and retention in the organic phase in the course of nanoparticle fabrication.

The release of paclitaxel from PBCA nanoparticles showed a clear biphasic release pattern (Fig. 4), largely as a result of diffusion of the paclitaxel molecules from the nanoparticles and only partially attributed to polymer degradation. As long as the polymer surface exists, diffusion is the main contributor, and the drug release is not completed until the total degradation of the polymer particles. Furthermore, the incorporation of lecithin and dextran 70 in the formulation may reduce the surface porosity of the nanoparticles, resulting in a significant slowdown of drug release and flattening of the release profile (33).

Paclitaxel-loaded PBCA nanoparticles showed cytotoxicity against A2780 cells 17 times higher than free paclitaxel, a finding similar with previous studies. This might be partially related to phagocytosis of the nanoparticles by the cancer cells during rapid cell proliferation (13). The drug-loaded PBCA nanoparticles were also found to exhibit a stronger cytotoxic effect than free paclitaxel against the resistant cancer cells (A2780/T) in the tested concentration range (Fig. 5), possibly due to the fact that this drug delivery system acts as a reservoir for paclitaxel to allow sustained drug release and protects paclitaxel from epimerization and hydrolysis (34,35) to maintain its activity. The enhanced cytotoxicity of the drug-loaded PBCA nanoparticles may also be associated with markedly increased accumulation of the nanoparticles in the cells

(36) and their entrapment in the endosomes/lysosomes following their intracellular entry to render the drug inaccessible for P-gp. In addition, it may be that the subsequent release of large quantities of paclitaxel from the endosomes/lysosomes overwhelms P-gp efflux (37,38).

The prior study suggested that doxorubicin-loaded PBCA nanoparticles enhanced the cytotoxicity against resistant cells due to the formation of an ion-pair complex between doxorubicin and a degradation product of PBCA. As paclitaxel is basically a neutral molecule impossible to form the ion pair complex, this mechanism can be dismissed for paclitaxel-loaded PBCA nanoparticles (23).

It was reported that some surfactants could reverse the activity of P-gp and multidrug resistance-associated protein 2 (MRP2) (39). Lecithin itself is a constituent component of the cell membrane involved in drug resistance, and it modifies the drug resistance profile by altering the exposure or function of P-gp (40). Calcein AM is a non-fluorescent substrate of P-gp which, once in the cells, is irreversibly converted by cytosolic esterase to calcein, a nonpermeable and fluorescent molecule (41). Therefore, the increased intracellular fluorescence of calcein in P-gp-overexpression cells exposed to drug-loaded PBCA nanoparticles and blank PBCA nanoparticles stated the inhibition of P-gp function. Short-term incubation of the cells with paclitaxel-loaded PBCA nanoparticles and blank PBCA nanoparticles caused a dose-dependent decrease in P-gp transport activity. Lecithin displayed an interesting effect that P-gp activity was increased at low lecithin concentrations while decreased at high concentrations, possibly because low concentration of lecithin induces P-gp phosphorylation and enhances its transporter activity (42). Based on these results, it might be concluded that the nanoparticle system with or without drug loading, rather than the surfactants, takes effect to reduce the MDR of the cancer cells.

Some researchers (13) hypothesized that paclitaxel-loaded nanoparticles may alter the composition and fluidity of the cell membrane, thereby altering the activity of P-gp, or activating the intracellular signal transduction mechanism(s) to down-regulate P-gp expression. Nevertheless, the regulation of P-gp expression is a complex process which involves multiple signal transduction pathways. Although paclitaxel-loaded PBCA nanoparticles and the free drug both presented the inhibition of MDR-1 mRNA expression in A2780/T cells, the statistical analysis failed to indicate a significant difference from the control level ($P > 0.05$, Fig. 7). Also, QRT-PCR analysis demonstrated that the blank nanoparticles and lecithin could not affect the expression of P-gp genes. Accumulating results revealed that paclitaxel-loaded PBCA nanoparticles enhanced the cytotoxicity in A2780/T cells by inhibiting P-gp function, but their effect on the expression of P-gp needs further investigation.

CONCLUSION

We prepared paclitaxel-loaded PBCA nanoparticles by interfacial polymerization to overcome MDR in human ovarian cancer cells. The data showed that these nanoparticles produced a significantly higher cytotoxicity than free paclitaxel against A2780/T cells by inhibiting P-gp function rather than obviously affecting the expression of MDR1 mRNA. In particular, the current study suggests that the reduction of MDR by paclitaxel-loaded PBCA nanoparticles is attributed to nanopaticle system effect irrelevant to the surfactant. The effect of the drug delivery system on P-gp expression still awaits further investigation.

ACKNOWLEDGMENTS

This work was supported by a grant from the National Natural Science Foundations of China (No30572361). The authors would like to thank Dr. XM Chen (Department of Occupational Hygiene, Southern Medical University) and Dr. XC Bai (Department of Cell Biology, School of Basic Medical Sciences, Southern Medical University) for technical assistance.

REFERENCES

1. Rogers BB. Taxol: a promising new drug of the '90s. Oncol Nurs Forum. 1993;20:1483–9.
2. Singla AK, Garg A, Aggarwal D. Paclitaxel and its formulations. Int J Pharm. 2002;235:179–92.
3. Liggins RT, Hunter WL, Burt HM. Solid-state characterization of paclitaxel. J Pharm Sci. 1997;86:1458–63.
4. Gelderblom H, Verweij J, Nooter K, Sparreboom A, Cremophor EL. The drawbacks and advantages of vehicle selection for drug formulation. Eur J Cancer. 2001;37:1590–8.
5. Yusuf RZ, Duan Z, Lamendola DE, Penson RT, Seiden MV. Paclitaxel resistance: molecular mechanisms and pharmacologic manipulation. Curr Cancer Drug Targets. 2003;3(1):1–19.
6. Calderwood SK, Khaleque MA, Sawyer DB, Ciocca DR. Heat shock proteins in cancer: chaperones of tumorigenesis. Trends Biochem Sci. 2006;31:164–72.
7. Kirkin V, Joos S, Zörnig M. The role of Bcl-2 family members in tumorigenesis. Biochim Biophys Acta. 2004;1644:229–49.
8. Szakács G, Paterson JK, Ludwig JA, Booth-Genthe C, Gottesman MM. Targeting multidrug resistance in cancer. Nat Rev Drug Discov. 2006;5:219–34.
9. O'Connor R. The pharmacology of cancer resistance. Anticancer Res. 2007;27:1267–72.
10. Stein WD, Bates SE, Fojo T. Intractable cancers: the many faces of multidrug resistance and the many targets it presents for therapeutic attack. Curr Drug Targets. 2004;5:333–46.
11. Cuvier C, Roblot-Treupel L, Millot JM, Lizard G, Chevillard S, Manfait M, *et al.* Doxorubicin-loaded nanospheres bypass tumor cell multidrug resistance. Biochem Pharmacol. 1992;44:509–17.
12. Soma CE, Dubernet C, Barratt G, Ne´mati F, Appel M, Benita S, *et al.* Ability of doxorubicin-loaded nanoparticles to overcome multi-drug resistance of tumor cells after their capture by macrophages. Pharm Res. 1999;16:1710–6.

13. Önyüksel H, Jeon E, Rubinstein I. Nanomicellar paclitaxel increases cytotoxicity of multidrug resistant breast cancer cells. Cancer Letters. 2009;274:327–30.
14. Minko T, Kopeckova P, Pozharov V, Kopecek J. HPMA copolymer bound adriamycin overcomes MDR1 gene encoded resistance in a human ovarian carcinoma cell line. J Control Release. 1998;54:223–33.
15. Huang CY, Chen CM, Lee YD. Synthesis of high loading and encapsulation efficient paclitaxel-loaded poly(n-butyl cyanoacrylate) nanoparticles via miniemulsion. Int J Pharm. 2007;338:267–75.
16. Couvreur P, Kante B, Lenaerts V, Scailteur V, Roland M, Speiser P. Tissue distribution of antitumor drugs associated with polyalkylcyanoacrylate nanoparticles. J Pharm Sci. 1980;69:199–202.
17. Couvreur P, Fattal E, Alphandary H, Puisieux F, Andremont A. Intracellular targeting of antibiotics by means of biodegradable nanoparticles. J Control Release. 1992;19:259–67.
18. Damge C, Michel C, Aprahamian M, Couvreur P, Devissaguet JP. Nanocapsules as carriers for oral peptide delivery. J Control Release. 1990;13:233–39.
19. Tasset Ch, Barette N, Thysman S, Ketelslegers JM, Lemoine D, Preat V. Polyisobutylcyanoacrylate nanoparticles as sustained release system for calcitonin. J Control Release. 1995;33:23–30.
20. Li Y, Ogris M, Wagner E, Pelisek J, Rüffer M. Nanoparticles bearing polyethyleneglycol-coupled transferrin as gene carriers: preparation and *in vitro* evaluation. Int J Pharm. 2003;259:93–101.
21. Ne´mati F, Dubernet C, de Verdière AC, Pouponb MF, Treupel-Acarc L, Puisieux F, *et al.* Some parameters influencing cytotoxicity of free doxorubicin and doxorubiicn-loaded nanoparticles in sensitive and multidrug resistant leucemic murine cells: incubation time, number of nanoparticles per cell. Int J Pharm. 1994;102:55–62.
22. de Verdière AC, Dubernet C, Némati F, Soma E, Appel M, Ferté J, *et al.* Reversion of multidrug resistance with polyalkylcyanoacrylate nanoparticles: towards a mechanism of action. Br J Cancer. 1997;76:198–205.
23. Dong X, Mattingly CA, Tseng MT, Cho MJ, Liu Y, Adams VR, *et al.* Doxorubicin and paclitaxel-loaded lipid-based nanoparticles overcome multidrug resistance by inhibiting P-glycoprotein and depleting ATP. Cancer Res. 2009;69:3918–26.
24. Zhang Y, Tang L, Sun L, Bao J, Song C, Huang L, *et al.* A novel paclitaxel-loaded poly(epsilon-caprolactone)/Poloxamer 188 blend nanoparticle overcoming multidrug resistance for cancer treatment. Acta Biomater. 2010;6:2045–52.
25. Ravindran J, Nair HB, Sung B, Prasad S, Tekmal RR, Aggarwal BB. Thymoquinone poly (lactide-co-glycolide) nanoparticles exhibit enhanced anti-proliferative, anti-inflammatory, and chemosensitization potential. Biochem Pharmacol. 2010;79:1640–7.
26. Wong HL, Rauth AM, Bendayan R, Manias JL, Ramaswamy M, Liu Z, *et al.* A new polymer-lipid hybrid nanoparticle system increases cytotoxicity of doxorubicin against multidrug-resistant human breast cancer cells. Pharm Res. 2006;23:1574–85.
27. Wong HL, Bendayan R, Rauth AM, Xue HY, Babakhanian K, Wu XY. A mechanistic study of enhanced doxorubicin uptake and retention in multi-drug resistant breast cancer cells using a polymer-lipid hybrid nanoparticle system. J Pharmacol Exp Ther. 2006;317:1372–81.
28. Chavanpatil MD, Patil Y, Panyam J. Susceptibility of nanoparticle-encapsulated paclitaxel to P-glycoprotein-mediated drug efflux. Int J Pharm. 2006;320:150–6.
29. Hekmatara T, Gelperina S, Vogel V, Yang SR, Kreuter J. Encapsulation of water-insoluble drugs in poly(butyl cyanoacrylate) nanoparticles. J Nanosci Nanotechnol. 2009;9:5091–8.
30. Polli JW, Wring SA, Humphreys JE, Huang L, Morgan JB, Webster LO, *et al.* Rational use of *in vitro* P-glycoprotein assays in drug discovery. J Pharmacol Exp Ther. 2001;299:620–8.
31. Susa M, Iyer AK, Ryu K, Hornicek FJ, Mankin H, Amiji MM, *et al.* Doxorubicin loaded polymeric nanoparticulate delivery system to overcome drug resistance in osteosarcoma. BMC Cancer. 2009;9:399.
32. Mitra A, Lin S. Effect of surfactant on fabrication and characterization of paclitaxel-loaded polybutylcyanoacrylate nanoparticulate delivery systems. J Pharm Pharmacol. 2003;55:895–902.
33. Mu L, Feng SS. Fabrication, characterization and *in vitro* release of paclitaxel (Taxol) loaded poly (lactic-co-glycolic acid) microspheres prepared by spray drying technique with lipid/cholesterol emulsifiers. J Control Release. 2001;76:239–54.
34. Slichenmyer WJ, Von Hoff DD. Taxol: a new and effective anticancer drug. Anticancer Drugs. 1991;2:519–30.
35. Dordunoo SK, Burt HM. Solubility and stability of taxol: effects of buffers and cyclodextrins. Int J Pharm. 1996;133:191–201.
36. He M, Zhao Z, Yin L, Tang C, Yin C. Hyaluronic acid coated poly(butyl cyanoacrylate) nanoparticles as anticancer drug carriers. Int J Pharm. 2009;373:165–73.
37. Brigger I, Dubernet C, Couvreur P. Nanoparticles in cancer therapy and diagnosis. Adv Drug Deliv Rev. 2002;54(5):631–51.
38. Larsen AK, Escargueil AE, Skladanowski A. Resistance mechanisms associated with altered intracellular distribution of anticancer agents. Pharmacol Ther. 2000;85(3):217–29.
39. Bogman K, Erne-Brand F, Alsenz J, Drewe J. The role of surfactants in the reversal of active transport mediated by multidrug resistance proteins. J Pharm Sci. 2003;92:1250–61.
40. Lo YL. Phospholipids as multidrug resistance modulators of the transport of epirubicin in human intestinal epithelial Caco-2 cell layers and everted gut sacs of rats. Biochem Pharmacol. 2000;60:1381–90.
41. Bauer B, Miller DS, Fricker G. Compound profiling for P-glycoprotein at the blood-brain barrier using a microplate screening system. Pharm Res. 2003;20:1170–6.
42. Mitsunaga Y, Takanaga H, Matsuo H, Naito M, Tsuruo T, Ohtani H, *et al.* Effect of bioflavonoids on vincristine transport across blood-brain barrier. Eur J Pharmacol. 2000;395:193–201.